Water Science & Technology

Model-based identification and testing of appropriate strategies to minimize N$_2$O emissions from biofilm deammonification

A. Freyschmidt (iD)* and M. Beier **IWA**

Institute for Sanitary Engineering and Waste Management (ISAH) of the Leibniz University Hannover, Welfengarten 1, Hannover 30167, Germany
*Corresponding author. E-mail: freyschmidt@isah.uni-hannover.de

(iD) AF, 0000-0003-3979-0006

ABSTRACT

Based on a one-year pilot plant operation of a two-step biofilm nitritation-anammox pilot plant, N$_2$O mitigation strategies were identified by applying a newly developed biofilm modeling approach. Due to adapted plant operation, the N$_2$O emission could be diminished by 75% (8.8% → 2.3% of NH$_4$-N$_{oxidized\_AOB}$). The results (measurement and simulation) confirm the huge importance of denitrification as an N$_2$O source or N$_2$O sink, depending on the boundary conditions. A significant reduction of N$_2$O emissions could only be achieved with a one-step deammonification system, which is related to low nitrite and HNO$_2$ concentrations. Increased oxygen concentrations in the bulk phase are not related to decreased emissions. N$_2$O formation by ammonium-oxidizing bacteria (AOB) just shifts deeper into the biofilm; zones with low oxygen concentrations are not avoidable in biofilm systems. Low oxygen concentrations in the bulk phase, however, result in a reduction of the total net N$_2$O formation due to increased activity of heterotrophic bacteria directly at the source of N$_2$O formation (outer biofilm layer). For the model-based identification of mitigation strategies, the standard modeling approaches for biofilms were expanded by including the factor-based N$_2$O formation and emission approach. The new model 'Biofilm/N$_2$O$_{ISAH}$' was successfully validated using data from pilot-scale measurement campaigns. Altogether, the investigation confirms that the employed digital model can strongly support the development of N$_2$O mitigation strategies without the need for specialized measurement inside the biofilm.

Key words: aeration strategies, control algorithms, denitrification, GHG Emissions

HIGHLIGHTS

- Modeling provides deeper insights into the dynamics of N$_2$O formation, conversion, and emission in biofilms.
- N$_2$O emission rates of biofilm systems are limited by diffusion rates.
- N$_2$O degradation mainly depends on the concentrations of oxygen and HNO$_2$.
- Ambivalent role of oxygen concentration: Lower concentrations promote heterotrophic N$_2$O denitrification, but increase N$_2$O formation by AOB.

INTRODUCTION

N$_2$O is a strong greenhouse gas (global warming potential = 265 CO$_2$ equivalents, IPCC 2013) that is also formed and released during biological nitrogen removal at wastewater treatment plants. Especially, highly loaded part stream systems with high ammonium conversion rates are affected. For this reason, the development of plant-specific and load-adapted strategies to reduce N$_2$O emissions is of high importance. In recent years, the existing knowledge on N$_2$O formation and emission has been applied to develop different N$_2$O mitigation strategies including covering of reactors (Vogel 2018), off-gas treatment in biofilters (Yoon *et al.* 2017), and adapted aeration control (Peng *et al.* 2017; Liu *et al.* 2021).

It can be assumed that high-performance processes cannot be operated without N$_2$O formation. In this context, the heterotrophic denitrification has a high potential as an N$_2$O sink (Beier *et al.* 2016, 2021; Vogel 2018), allowing the reduction of N$_2$O formed by ammonium-oxidizing bacteria (AOB) via incomplete hydroxylamine oxidation and autotrophic denitrification. For this reason, providing sufficient denitrification capacities (anoxic environments) plays a key role in reducing N$_2$O emissions. This is where biofilm systems are advantageous, as anoxic zones can be established regardless of the aeration

strategy (Ye *et al.* 2022). Besides oxygen, nitrous acid (HNO_2) strongly influences the sub-process of N_2O reduction. N_2O accumulation can be observed, when an HNO_2 concentration of 0.001 mg HNO_2-N/l is exceeded (Vogel 2018).

For the selection of an appropriate mitigation strategy, it is essential to clearly identify the site-specific process steps and boundary conditions that cause N_2O formation. However, a separation between N_2O formation, conversion, and gas transfer is difficult to realize only relying on measurement data. In particular, processes in biofilms cannot be distinguished using standard measurement methods. In this context, mathematical modeling can serve as a supporting tool, enabling deeper insights into N_2O formation and emission mechanisms as well as testing and comparison of measures before the full-scale implementation.

For suspended biomass systems, N_2O formation and conversion can already be predicted quite precisely (Ye *et al.* 2022). N_2O formation related to AOB can be modeled by relying on a biological description of hydroxylamine oxidation pathway and autotrophic denitrification (e. g. Ni *et al.* 2014). Other approaches are based on formation factors (Beier *et al.* 2021). The heterotrophic denitrification is commonly split into three (Schulthess & Gujer 1996; Beier *et al.* 2021) or four (Hiatt & Grady 2008) sub-processes. However, there are also approaches including the indirect coupling of electrons (Pan *et al.* 2013; Ni *et al.* 2014). To calculate emissions from (net) formation, a gas transfer model is additionally required, usually based on the ideal gas equation and Henry's law (e.g. Beier *et al.* 2021).

For biofilm systems, transport mechanisms inside the biofilm have to be considered in addition to the biological processes. Diffusive transport can already be described relatively precisely using zero-order (average over depth) or first-order rates; however, more complex 2D or 3D approaches also exist (Pérez *et al.* 2005; Rittmann *et al.* 2018). In the case of variable biofilm thickness, attachment or detachment of particulate matter and biomass must also be included; for example, fixed attachment or detachment rates are used (Rittmann *et al.* 2018). More detailed models represent the attachment and detachment of individual bacterial cells (Wang & Bryers 1997).

The biofilm can be modeled as a zero-, one-, two- or three-dimensional system. While zero-dimensional models assume a homogeneous biofilm structure, local boundary conditions (substrate availability, oxygen concentration, biomass concentration, and composition…) vary in one- to three-dimensional models. For engineering applications, 1D models only considering variations over the biofilm thickness are generally considered sufficiently accurate (Pérez *et al.* 2005; Rittmann *et al.* 2018). The one-dimensional biofilm is usually divided into several layers, each of which is assumed to be completely mixed (Rittmann *et al.* 2018). 2D or 3D models can be implemented as variable volume continuum, cellular automata, or individual biomass models (Alpkvist *et al.* 2006; Rittmann *et al.* 2018); in research, neural networks and deep learning processes are also applied (Shi & Xu 2018).

In this study, a biofilm model of a pilot-scale deammonification plant was created and combined with an expanded ASM model developed by Beier *et al.* (2021) to compute N_2O emissions. The model was applied to investigate the dynamics of N_2O formation, conversion, and emission independently from each other inside the biofilm. Based on these findings, different N_2O mitigation strategies were developed and evaluated.

MATERIAL AND METHODS

Pilot plant

The pilot plant consists of two covered reactors arranged in series each having a volume of 220 l. The gas volume between the water surface and the reactor cover is approximately 10 l. Both reactors are equipped with textile biofilm carriers (Cleartec® BioCurlz, Jäger, Germany) providing a theoretical surface for biofilm growth of 141 m² per reactor. The first reactor was planned to be operated as partial nitration and is intermittently aerated (30 min on/ 30 min off) to suppress NOB growth. In the second reactor, anaerobic ammonium oxidation took place. In the following evaluations, however, only the nitration reactor is investigated, since anammox bacteria do not contribute to either N_2O formation or N_2O conversion (Kartal *et al.* 2011; Schneider *et al.* 2011). Additionally to the direct aeration of the reactor, the recirculation flow can also be aerated (indirect aeration). A flow scheme of the pilot plant is shown in Figure 1.

Both reactors are equipped with online temperature sensors; in the nitration reactor, an online pH sensor and an online oxygen sensor are additionally installed. NH_4-N, NO_2-N, NO_3-N, alkalinity, COD, and $COD_{filtered}$ are weekly measured with cuvette tests (Hach, Germany). In single measurement campaigns, N_2O was determined in the nitration reactor in the water phase (sensor installed in measurement cell in the outflow) and gas phase (sensor installed in the off-gas outlet) employing
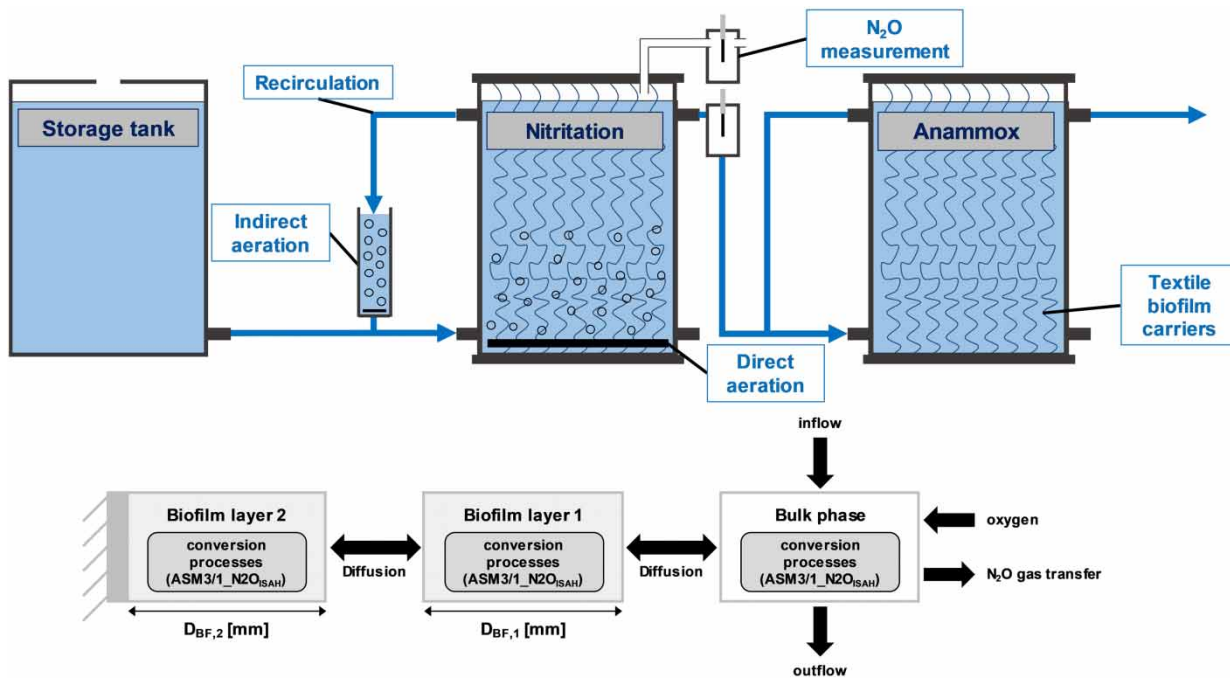
Figure 1 | Flow scheme of the pilot plant and biofilm model.

Clark-type N_2O microsensors (Unisense, Denmark). The gas volume flow was calculated based on the gas velocity measured at the off-gas outlet.

The measurement campaign that is used to validate the ASM model took place in week 24 of operation. In this operation phase, the plant was fed with 120 l of sludge water from a nearby large-scale wastewater treatment plant (mean composition: $C_{NH4-N} = 800$ mg NH_4-N/l, alkalinity $= 30$ mmol/l, COD/N $= 0.4$) resulting in an ammonium load of 96 g NH_4-N/d and 0.44 kg NH_4-N/m³/d, respectively. The pH value in the nitritation reactor was 5.8, the temperature was 27.2 °C, and the oxygen concentration in the liquid phase was 1.5 mg/l during the aerated phase. High N_2O emissions are expected due to high NH_4 conversion rates (highly loaded system) and high nitrite concentrations.

Starting in week 20, an increasing activity of anammox was observed in the first reactor (total one-step deammonification was reached after 32 weeks), so that not only nitrogen conversion (NH_4-N$\rightarrow$ NO_2-N), but also nitrogen removal took place. This can be taken as evidence that there are anoxic zones within the biofilm allowing anaerobic ammonium oxidation and denitrification.

Five scenarios were implemented and evaluated for their potential to reduce N_2O emissions. The boundary conditions varied for each scenario are summarized in Table 1. For the modeling study, only those parameters were selected that on

Table 1 | Varied boundary conditions for each scenario (deamm.: deammonification, interm.: intermittent aeration, cont.: continuous aeration, bold: changes compared to baseline scenario)

scenario	process	aeration	pH
baseline	nitritation	direct interm. (1.5 mg/l)	5.8
S1	**one-step deamm.**	direct interm. (1.5 mg/l)	5.8
S2	**one-step deamm.**	direct interm. (1.5 mg/l)	**7.0**
S3	nitritation	**direct interm. (3 mg/l)**	5.8
S4	nitritation	**indirect cont. (1.5 mg/l)**	5.8
S5	**one-step deamm.**	**indirect cont. (1.5 mg/l)**	**7.0**

the one hand can be easily modified during operation and on the other hand have a strong impact on N_2O formation by denitrification. The dosage of additional carbon was not considered, as its influence is only relevant for substrate-limited conditions. Moreover, as the N_2O load is low compared to the total N load, the organic C released from the hydrolysis of dead biomass is expected to be sufficient for N_2O denitrification.

Biological model and gas transfer model

The ASM model employed in this study is briefly described below; more information can be extracted from Beier *et al.* 2021. Nitrification is depicted as a two-step process (NH_4-N$\rightarrow$ NO_2-N$\rightarrow$ NO_3-N) and denitrification as a three-step process (NO_3-N $\rightarrow NO_2$-N $\rightarrow N_2O$-N $\rightarrow N_2$). Moreover, the biological process of anaerobic ammonium oxidation is included. The inhibiting effects of HNO_2 and NH_3 on autotrophic and heterotrophic (only HNO_2) microorganisms are considered as well. N_2O formation is calculated as a fraction of converted NH_4, relying on dynamic N_2O formation factors depending on the NH_4-N conversion rate and the concentrations of NO_2-N and O_2. N_2O transfer to the gaseous phase considers diffusion according to Henry's law as well as aeration-related gas stripping.

RESULTS AND DISCUSSION

A combined modeling approach for N_2O emissions of biofilm systems

A digital model of the pilot plant was developed using the software SIMBA# (ifak, Germany). For this purpose, it was necessary to combine a modeling approach for biofilm with a biological model for the calculation of N_2O formation, conversion, and emission.

For biofilm modeling, the Simba# fixed-bed biofilm module was employed. The total reactor volume was split between an inert volume (biofilm support), the bulk volume, and the biofilm volume, which equals the product of biofilm carrier surface and biofilm thickness. Based on a predefined start value, the biofilm thickness is calculated dynamically for each simulation step depending on biomass growth as well as attachment and detachment rates. According to the modeling outcomes, a higher initial biofilm thickness resulted in a higher steady-state biofilm thickness with a larger anoxic zone promoting the growth of anammox and denitrifying biomass. For this reason, total NH_4 conversion increased faster, when a higher initial biofilm thickness was chosen. However, the biofilm thickness had only a minor influence on the total plant performance (total one-step deammonification), because conversion rates of AOB and NOB are limited by other boundary conditions like diffusion transport rates and alkalinity. Consequently, N_2O formation was also only slightly influenced by biofilm thickness.

Using a one-dimensional approach, the biofilm itself was subdivided into two fully stirred layers, which have interface areas to other biofilm elements and/or the bulk phase. With the selected approach, the varying environmental conditions in the different biofilm zones (especially aerobic/anoxic conditions) due to diffusion gradients can be represented with sufficient accuracy. In each biofilm layer and the bulk phase, the biological conversion processes are computed independently by applying the expanded ASM model ASM3/1_N_2O_{ISAH} developed by Beier *et al.* (2021). The transfer of dissolved substrates and reaction products between the different layers and the bulk phase is described by diffusion. The diffusion velocity of every ASM parameter is defined based on diffusion coefficients. The system model developed in this study is schematically depicted in Figure 1.

The operational data showed that it is necessary to integrate the slowly establishing deammonification as a dynamic process. The assumption of pure nitrification is not appropriate for biofilm systems. Best simulation results were achieved with a low start concentration of anammox bacteria in the nitritation reactor enabling slow growth of anammox biomass (anammox growth rate (0.072 d^{-1}) $<$ $<$AOB growth rate (2.05 d^{-1}) in the applied ASM model). Since the biofilm in the first reactor was started up as a continuously aerated nitrification system, the assumption of a low initial concentration is reasonable. With this approach, the fast development of nitritation followed by the slowly growing activity of the anammox microorganisms, which was observed in reality (indicated by decreasing NO_2 concentrations and increasing NH_4 conversion), can be depicted with adequate accuracy.

For model validation of the entire system (layered biofilm model + ASM model), measurement data and simulation results of two independent operational situations (nitritation and one-step deammonification) were compared. This study concentrates on strategy development. Therefore, all simulation studies are run from a defined (temporary) steady-state to ensure comparability of results (Modeling of dynamic states was beyond the scope of this study). As proved by Beier *et al.* (2021),

no adaption of the kinetic parameters or the calculation functions of N_2O formation factors is required, so the ASM model itself was considered validated.

Measured and simulated N_2O-N emissions as well as the N_2O emission rate related to NH_4 conversion are presented in Figure 2 for the first operational situation (nitritation). According to the measurement results, 1.95 g N_2O-N/d are emitted via the gas phase and 0.03 g N_2O-N/d via the water phase. This results in a mean emission factor (emitted N_2O-N load divided by NH_4-N load oxidized by AOB) of 8.8% of NH_4-$N_{oxidized\_AOB}$, which is in the upper range for highly loaded systems. However, higher emission factors for laboratory-scale or pilot-scale plants were reported (e.g. Peng *et al.* 2017). Using the model, similar emission loads (gas phase: 1.91 g N_2O-N/d; water phase: 0.03 g N_2O-N/d) are calculated. The stepped curve of N_2O emissions via the gas phase is due to intermittent aeration (very low emissions during the unaerated phase).

Moreover, the dynamics of the measured and simulated N_2O emission factors are shown in Figure 2 (it was assumed that NH_4 is only converted during the aerated phase). The measured simulation factor peaks at the beginning of the aerated phase, due to the fast stripping of N_2O accumulated in the unaerated phase. In the simulations, N_2O stripping velocity was lower; however, total emissions were identical. The simulated emission factor represents the mean value of the measured emission factor.

For the second validation data set (one-step deammonification), similar results were obtained (data not shown). The research outcomes confirm that the chosen modeling approach is suited to predict N_2O emissions for specific operational situations. The concept of using function-based N_2O formation factors can be applied to biofilm systems. Furthermore, the two-layered biofilm model is adequate to simulate the specific characteristics (especially biomass composition) of the investigated biofilm.

N_2O formation and emissions of the pilot plant (baseline scenario)

The results of the modeling outcomes are summarized in Figure 3 (left: biofilm layer 2, mid: biofilm layer 1, right: bulk phase). Concentrations of O_2, HNO_2, and N_2O (diagrams), as well as the roles of AOB and heterotrophic bacteria regarding N_2O during the aerobic as well as the anoxic phase (grey boxes), are given for both biofilm layers and the bulk phase. Moreover, the black arrows indicate the direction of N_2O diffusion.

According to the simulation outcomes, AOB activity is mainly related to the outer biofilm layer (93% of oxidized ammonium). During the aerated phase, an O_2 concentration between 0.2 and 0.25 mg/l is maintained in that layer. The N_2O formation factor is 8.0% (NH_4-N conversion-related formation factor = 2.7%; NO_2-N-related formation factor = 2.0%; O_2-related formation factor = 3.3%).

Formed N_2O diffuses to the bulk phase (high concentration gradient), where a sharp decrease of the N_2O concentration can be observed during the aerated period. This indicates that the N_2O emission rate is limited by the rate of N_2O transfer from the biofilm to the bulk phase. However, the N_2O concentration does not fall below 0.23 mg N_2O-N/l (according to measurement and simulation).

During the aerated phase, N_2O accumulates in the inner biofilm layer due to N_2O production by AOB, but also by heterotrophic bacteria (O_2 concentration <0.0003 mg/l). NO_2-N reduction rates are approximately 50 times higher than N_2O-N
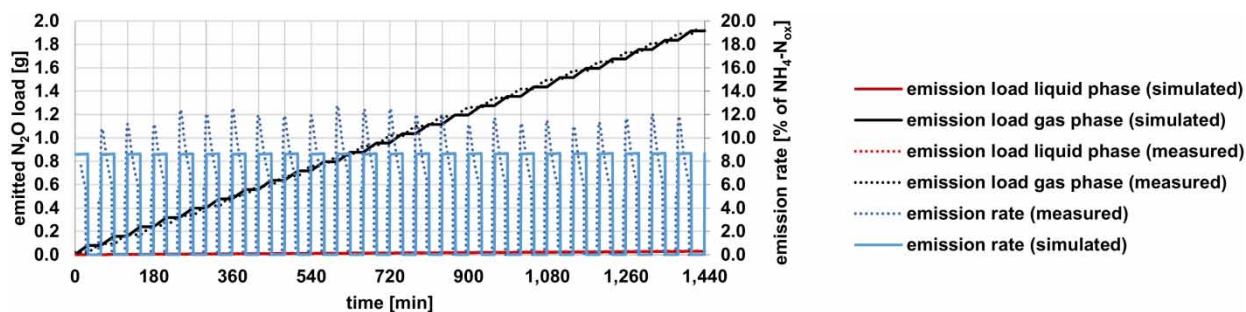

Figure 2 | Measured and simulated N_2O emission (combination of net N_2O formation and gas exchange) and resulting emission rate (g N_2O/g NH_4-N_{conv}/d).
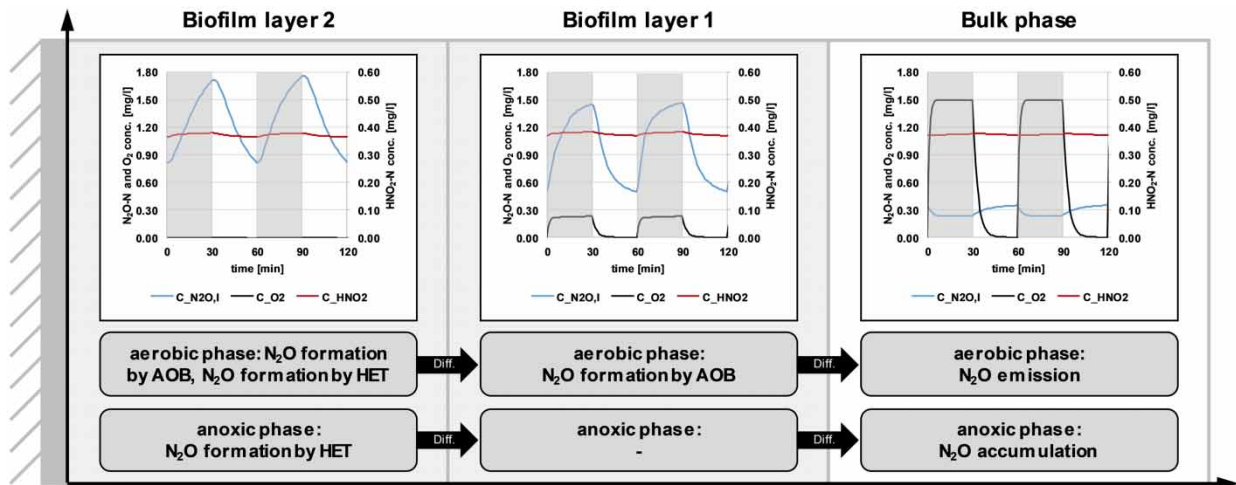
Figure 3 | Processes of N$_2$O formation, conversion, and emission in the aerobic and the anoxic phase and concentrations of N$_2$O-N, O$_2$, and HNO$_2$-N in the biofilm layers and the bulk phase for the baseline scenario (black arrows: direction of N$_2$O diffusion).

reduction rates. The low N$_2$O-N conversion rate can be traced back to high HNO$_2$-N concentrations (>0.37 mg HNO$_2$-N/l) exceeding the threshold for N$_2$O accumulation (0.001 mg HNO$_2$-N/l) by far. For this reason, N$_2$O denitrification is nearly completely inhibited. In total, the N$_2$O accumulation rate in the inner biofilm layer is 10-fold lower than in the outer biofilm layer. The slightly higher N$_2$O concentration can be traced back to a limited outward diffusion rate due to a small concentration gradient between both biofilm layers.

In the anoxic phase, AOB activity is very low due to a lack of oxygen. N$_2$O is transferred from layer 2 to layer 1 and from layer 1 to the bulk phase, so that the concentrations in both biofilm layers decrease and the concentration in the bulk phase increases. However, still much higher concentrations are maintained in the biofilm compared to the bulk phase. Due to inhibited (HNO$_2$) N$_2$O reduction, the decrease of N$_2$O concentration in the biofilm cannot be traced back to the activity of heterotrophic bacteria. In contrast, N$_2$O continues to be produced in the inner biofilm layer.

By setting the activity of heterotrophic bacteria related to N$_2$O formation and reduction to zero, the impact of denitrification on total N$_2$O formation was investigated. Neglecting the activity of heterotrophic bacteria, emitted N$_2$O load was slightly (0.19 g N$_2$O-N/d or 10%) decreased.

Summarizing the modeling outcomes for the baseline scenario, N$_2$O formation is mainly related to the activity of AOB in the outer biofilm layer during the aerobic phase. Denitrification plays a minor role as an N$_2$O source, but cannot act as an N$_2$O sink due to inhibition of N$_2$O reduction. Formed N$_2$O diffuses from the inner biofilm layer towards the bulk phase. The N$_2$O emission rate is limited by the gas transfer rate from the biofilm.

Evaluation of different measures to reduce N$_2$O emissions

Figure 4 summarizes the modeling outcomes of the investigated scenarios.

In Scenario S1 (one-step deammonification – reduced nitrite concentrations), N$_2$O is still mainly formed by AOB in the outer biofilm layer during the aerobic phase. Compared to the baseline scenario, the N$_2$O formation factor calculated by the model decreased by 2.8% due to the much lower nitrite concentrations (total formation factor = 5.2%).

Formed N$_2$O diffuses not only to the bulk phase but also to the inner biofilm layer. The reversal of the diffusion direction compared to the baseline scenario can be traced back to a changed concentration gradient. Moreover, N$_2$O re-transfer from the bulk phase to the biofilm can be observed at the end of the anoxic period, as the N$_2$O concentration in the outer biofilm layer falls below the concentration in the water phase. Consequently, the amount of N$_2$O that is stripped from the bulk phase is significantly reduced.

The modeling results show that heterotrophic bacteria do not contribute to N$_2$O formation anymore. In contrast, high N$_2$O conversion rates in the inner biofilm layer indicate that denitrification acts as an N$_2$O sink converting N$_2$O that is formed by AOB. HNO$_2$ inhibition can no longer be observed. Due to the low oxygen concentrations (<0.005 mg/l), N$_2$O reduction is
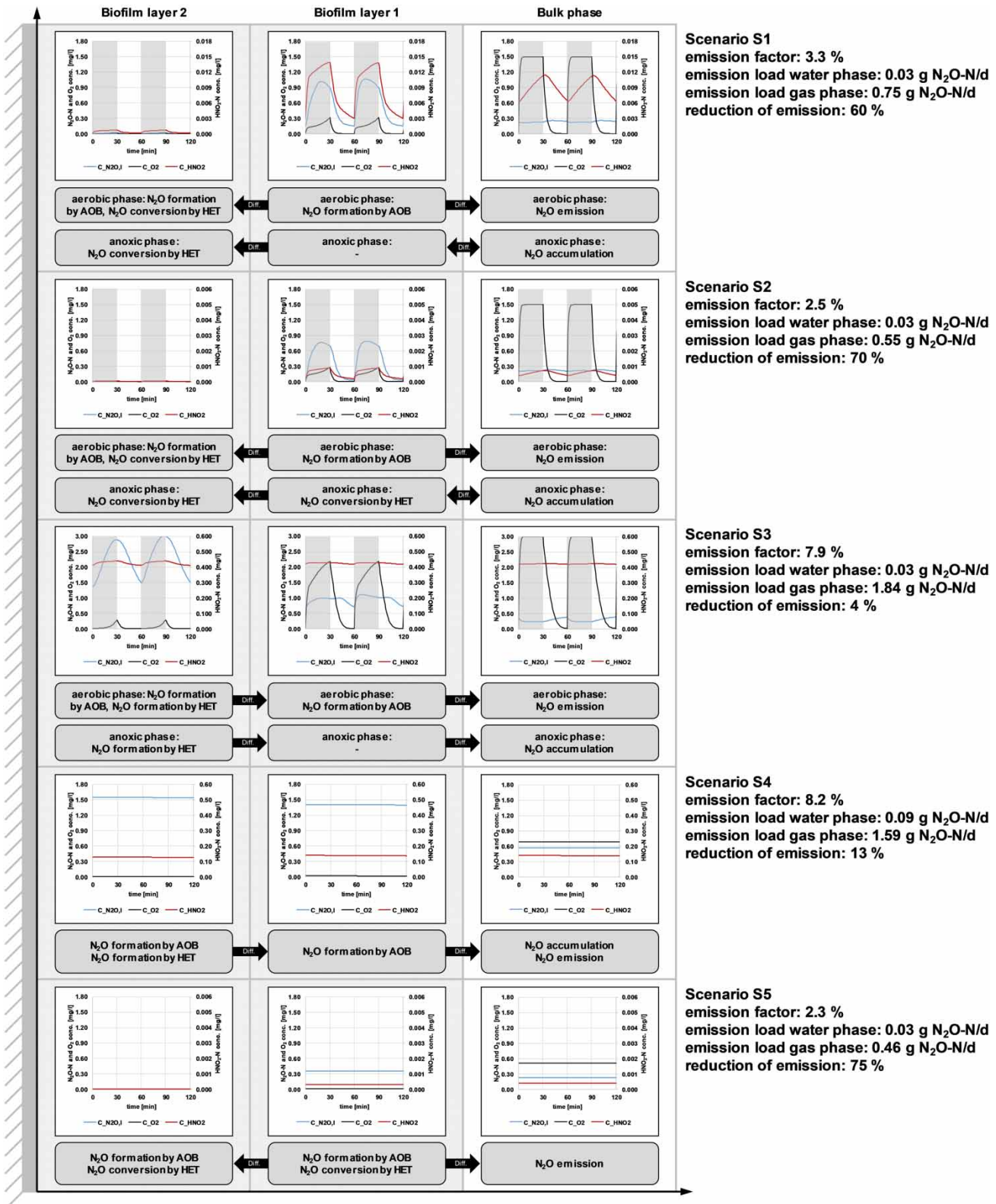
Figure 4 | Processes of N$_2$O formation, conversion, and emission in the aerobic and the anoxic phase and concentrations of N$_2$O-N, O$_2$, and HNO$_2$-N in the biofilm layers and the bulk phase for scenarios S1 – S5 (black arrows: direction of N$_2$O diffusion).

not directly affected by the aeration regime but is limited by N_2O availability in the anoxic phase (depending on the N_2O diffusion rate). Consequently, no N_2O accumulation can be observed in the inner biofilm layer, because the diffused N_2O is directly converted. HNO_2-N concentrations in the outer biofilm layer and the bulk phase still exceed the threshold for inhibition of N_2O denitrification, so the N_2O cannot be converted directly at the point of its formation.

Scenario S1 proves the high potential of one-step deammonification in biofilm systems concerning N_2O emission. By enabling N_2O denitrification in the inner biofilm layer, the amount of N_2O diffusing to the water phase significantly decreases. However, the N_2O reduction rate is limited by the diffusion rate.

Simulating with a pH value of 7.0 (Scenario S2) results in a decrease in total N_2O emissions by 26% compared to scenario S1 (a pH increase was also observed in the pilot plant after the establishment of full one-step deammonification). Unlike in the previous scenario, the HNO_2-N concentration causing N_2O accumulation is not exceeded anywhere in the reactor, so N_2O reduction can take place in all biofilm layers. However, O_2 inhibition of all denitrification sub-processes prevents N_2O reduction in the aerobic phase at least in the outer biofilm layer. Thus, in the outer biofilm layer, N_2O is formed in the aerobic phase and nearly completely denitrified in the anoxic phase. N_2O diffusing into the inner biofilm layer is immediately converted at any time so that the N_2O concentration is always below 0.004 mg N_2O-N/l. Analyzing the modeling results, it can be concluded that the emitted N_2O load mostly consists of N_2O diffusing to the bulk phase during the aerated phase. In the unaerated phase, N_2O re-transfer to the biofilm can be observed. At this state, a higher reduction of N_2O emissions can only be achieved by limiting the diffusion to the bulk phase or by preventing N_2O formation.

In Scenario S3 (increased oxygen concentration) the increased transfer of oxygen into the inner biofilm layer permitted a strong AOB activity throughout the biofilm during the aerated phase. Hence, N_2O is formed in both biofilm layers. While the N_2O formation factor in the outer biofilm layer decreased by 40% compared to the baseline scenario due to higher O_2 concentrations (N_2O formation factors related to NO_2 concentration and NH_4 conversion remained stable), an elevated N_2O formation factor ($>8\%$) was monitored in the inner biofilm layer. Consequently, the AOB-related N_2O formation decreased in the outer biofilm layer but increased in the inner biofilm layer.

The simulation results confirm that the heterotrophic microorganisms in the inner biofilm layer contribute to N_2O formation in both the aerobic and the anoxic phases. The O_2 concentration in the aerobic phase is not high enough to cause a serious inhibition of NO_2 reduction, but N_2O reduction is inhibited by high HNO_2 concentrations.

Altogether, higher O_2 concentrations alone cannot achieve a significant reduction of N_2O formation in biofilm systems, as there will always be a zone with low oxygen concentrations promoting N_2O formation by AOB. Stronger aeration could also be expected to increase N_2O formation due to elevated activity of AOB; however, AOB activity is already limited by alkalinity.

In scenario S4, the recirculation flow was continuously aerated instead of directly aerating the reactor. Thus, the time one liter of water is exposed to the airflow was reduced. Consequently, much higher concentrations were reached in the bulk phase as well as in the biofilm. However, N_2O emissions were only reduced by 13%, referring to the baseline scenario. This can be again explained by high HNO_2 concentrations in both biofilm layers, clearly exceeding the threshold for N_2O accumulation. So, the accumulated N_2O cannot be degraded. Moreover, an increase in the N_2O formation factor due to low oxygen concentrations in both biofilm layers was computed. Thus, reduced stripping does not provide a benefit in this scenario because the increased N_2O formation cannot be compensated by N_2O denitrification. However, the simulation outcomes confirm the general potential of applying indirect aeration systems.

The system can be optimized by altering the recirculation flow. A higher recirculation flow could increase the O_2 input; although a minimum retention time in the saturation column should be maintained. Moreover, higher recirculation rates also again increase N_2O emissions. A balance must be found between plant performance and mitigation of N_2O emissions.

Using indirect aeration in combination with one-step deammonification and increased pH value (Scenario S5), the N_2O emissions could be diminished by 16% compared to scenario S2. N_2O stripping was reduced, so that slightly higher N_2O concentrations in the liquid phase were achieved, resulting in smaller concentration gradients and diffusion rates. Moreover, N_2O concentration peaks like in the aerated phase of scenario S2 can be avoided, due to constantly low oxygen concentrations in both biofilm layers providing additional N_2O denitrification capacities.

In scenario S5, the recirculation flow also has a strong influence on the total emission reduction. Higher recirculation rates lead to higher emissions; however, if the recirculation flow is too high, higher emissions than in scenario S2 are observed, since the increased formation can no longer be compensated by lower stripping.

Summary of results

The results show that the developed modeling approach allows separating the processes of N_2O formation, conversion, and diffusion within the biofilm without measuring inside the biofilm. Autotrophic N_2O formation can be reproduced with sufficient accuracy using dynamic formation factors. In contrast, denitrification should be modeled as a biological process, since the specific local boundary conditions determine whether denitrification is a source or sink. Here, the HNO_2 concentration is confirmed as a major influencing factor. In this context, the model accuracy can be improved by a more precise calculation of the pH value. For biofilm systems, the correct simulation of O_2 penetration depth is also important for the development of aerobic and anoxic environments. Altogether, the model demonstrated its suitability for the development of appropriate mitigation strategies.

The emitted N_2O loads as well as the N_2O emission factors of the investigated scenarios are summarized in Figure 5.

The presented investigations emphasize the huge importance of denitrification as an N_2O source and N_2O sink. A significant reduction of N_2O emissions of the investigated plant could only be achieved in one-step deammonification systems, which are related to low nitrite and HNO_2 concentrations.

Increasing the oxygen concentrations in the bulk phase from 1.5 to 3 mg/l (biofilm layer 1: 0.25 → 2.1 mg/l, biofilm layer 2: 0.0 → 0.2 mg/l) is not related with significantly decreased emissions (scenario S3). Even though the N_2O formation can be slightly reduced in the outer biofilm layer, higher oxygen transfer lead to higher AOB activity in the inner biofilm layer (again low oxygen concentration). Altogether, low oxygen concentrations are not avoidable in biofilm systems. However, lower oxygen concentrations in the bulk phase (scenario S5) can improve the simultaneous denitrification performance. Although higher formation factors are observed, total net N_2O formation is reduced due to high activity of heterotrophic bacteria directly at the source of autotrophic N_2O formation. Indirect aeration alone just has an impact, if denitrification capacities are available. Otherwise, accumulated N_2O cannot be removed from the liquid phase. For the operated pilot plant and the given operational situation, lower O_2 concentrations are the more promising way to avoid emissions. However, these results are not universally valid but always depend on the local operating conditions.

As expected, carbon availability was found not to be a limiting factor due to the relatively low N_2O load (compared to the total N load). Just the biomass decay releases enough organic substrate.

In a two-stage system (nitritation reactor and anammox reactor), denitrification can additionally be established as an N_2O sink in the second, unaerated reactor. In this case, a transfer of the formed N_2O from nitritation to anammox reactor is essential; stripping must be minimized, and the presented system of indirect aeration has a high potential. Altogether, however, the single-stage operation is more advantageous (low nitrite concentrations, anoxic zones occur in the biofilm anyway, no N_2O stripping inside the biofilm) and will be achieved almost automatically with longer operation, due to growing of anammox in the inner biofilm layers.
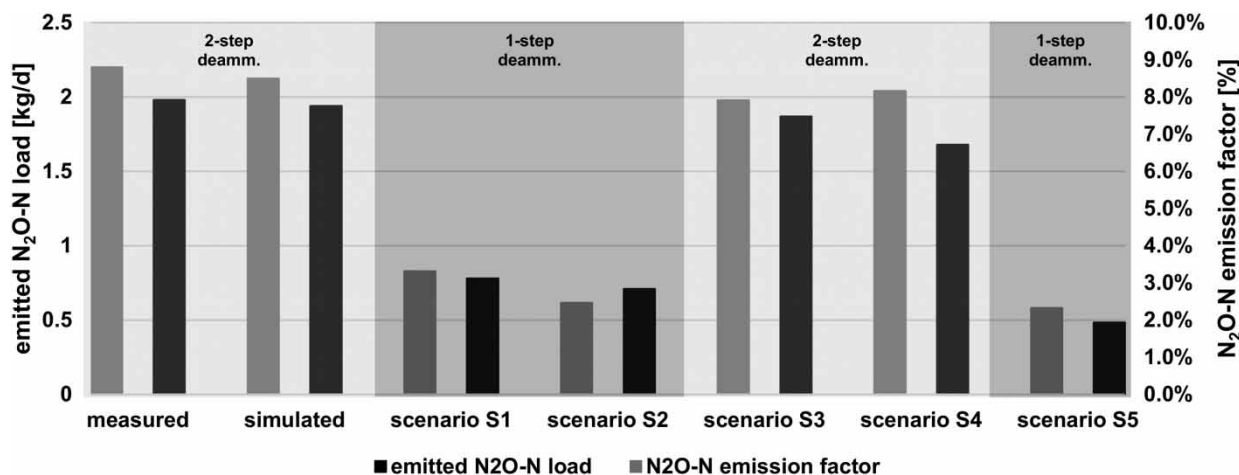

Figure 5 | Summary of results.

CONCLUSION

- It was proved that modeling can provide deeper insights into the dynamics of N_2O formation, conversion, and emission in the biofilm. For calibration, measurement of the N_2O concentration in the liquid phase and the off-gas is sufficient. The developed approach was successfully employed for the derivation and evaluation of N_2O mitigation strategies.
- N_2O emission rates in biofilm systems are driven by diffusion rates. The biofilm can serve as N_2O storage; only the N_2O that is transferred to the liquid phase can be emitted.
- N_2O degradation can be achieved permanently in the inner biofilm layers and temporarily in the outer biofilm layers (unaerated phase), depending on the concentrations of oxygen and HNO_2. A significant reduction of the N_2O emissions is possible if sufficient denitrification capacities (characterized by COD availability, anoxic environment, and non-inhibiting HNO_2 concentrations) are provided. Enough organic substrate is released from biomass decay.
- The modeling outcomes demonstrate that, due to concentration gradients, better conditions for heterotrophic N_2O denitrification could be achieved in the inner biofilm layer. It was confirmed that the HNO_2 concentration is a key parameter that determines whether heterotrophic denitrification is a source or a sink of N_2O. The model accuracy can further be improved by additionally including the pH value as a variable.
- Measurement and modeling results show that the oxygen concentration plays an ambivalent role: Lower concentrations promote heterotrophic N_2O denitrification, but increase N_2O formation by AOB. The optimal concentration (regarding N_2O emissions) has to be identified for specific operational situations. In this study, lower N_2O emissions were achieved with lower oxygen concentrations.

DATA AVAILABILITY STATEMENT

All relevant data are included in the paper or its Supplementary Information.

CONFLICT OF INTEREST

The authors declare there is no conflict.

REFERENCES

Alpkvist, E., Picioreanu, C., van Loosdrecht, M. C. M. & Heyden, A. 2006 Three-dimensional biofilm model with individual cells and continuum EPS matrix. *Biotechnology and Bioengineering* **94** (5), 961–979. doi:10.1002/bit.20917.

Beier, M., Schneider, Y. & Vogel, B. 2016 Factors influencing nitrous oxide reduction by denitrification as a means to minimize greenhouse gas emissions. In *IWA Specialist Conference Microbial Ecology and Water Engineering*, 2016, Copenhagen, Denmark.

Beier, M., Feldkämper, I. & Freyschmidt, A. 2021 Model assisted identification of N2O mitigation strategies for full-scale reject water treatment plants. *Water Science and Technology* **39** (6), 349–363. doi:10.2166/wst.2021.141.

Hiatt, W. C. & Grady, C. P. L. 2008 An updated process model for carbon oxidation, nitrification and denitrification. *Water Environment Research* **80** (11), 2145–2156. doi:10.2175/106143008X304776.

IPCC 2013 *IPCC 5th Assessment Report: The Physical Science Basis*. Cambridge University Press, Cambridge, UK. and New York, NY, USA.

Kartal, B., Maalcke, W. J., de Almeida, N. M., Cirpus, I., Gloerich, J., Geerts, W., op den Camp, H. J. M., Harhangi, H. R., Janssen-Megens, E. M., Francoijs, K.-J., Stunnenberg, H. G., Keltjens, J. T., Jetten, M. S. M. & Strous, M. 2011 Molecular mechanism of anaerobic ammonium oxidation. *Nature* **479**, 127–130. doi:10.1038/nature10453.

Liu, T., Liu, S., He, S., Tian, Z. & Zheng, M. 2021 Minimization of N2O emission through intermittent aeration in a Sequencing Batch Reactor (SBR): main behavior and mechanism. *Water* **13** (2), 210. doi:10.3390/w13020210.

Ni, B.-J., Peng, L., Law, Y., Guo, J. & Yuan, Z. 2014 Modelling of nitrous oxide production by autotrophic ammonia-oxidizing bacteria with multiple production pathways. *Environmental Science & Technology* **47** (14), 7795–7803. doi:10.1021/es405592h.

Pan, Y., Ni, B.-J. & Yuan, Z. 2013 Modeling electron competition among nitrogen oxides reduction and N2O accumulation in denitrification. *Environmental Science & Technology* **47**, 11083–11091. doi:10.1021/es402348n.

Peng, L., Carvajal-Arroyo, J. M., Seuntjens, D., Prat, D., Colica, G., Pintucci, C. & Vlaeminck, S. E. 2017 Smart operation of nitritation/denitritation virtually abolishes nitrous oxide emission during treatment of co-digested pig slurry centrate. *Water Research* **127**, 1–10. doi:10.1016/j.watres.2017.09.049.

Pérez, J., Picioreanu, C. & van Loosdrecht, M. 2005 Modeling biofilm and floc diffusion processes based on analytical solution of reaction-diffusion equations. *Water Research* **39** (7), 1311–1323. doi:10.1016/j.watres.2004.12.020.

Rittmann, B. E., Boltz, J. P., Brockmann, D., Daigger, G. T., Morgenroth, E. & Sørensen, K. 2018 A framework for good biofilm reactor modeling practice (GBRMP). *Water Science and Technology* **77** (5–6), 1149–1164. doi:10.2166/wst.2018.021.

Schneider, Y., Beier, M. & Rosenwinkel, K.-H. 2011 Determination of the nitrous oxide emission potential of deammonification under anoxic conditions. *Water Environment* **83** (12), 2199–2210. doi:10.2175/106143011X13173281922437.

Schulthess, R. V. & Gujer, W. 1996 Release of nitrous oxide (N2O) from denitrifying activated sludge: verification and application of a mathematical model. *Water Research* **30** (3), 521–530. doi:10.1016/0043-1354(95)00204-9.

Shi, S. & Xu, G. 2018 Novel performance prediction model of a biofilm system treating domestic wastewater based on stacked denoising auto-encoders deep learning network. *Chemical Engineering Journal* **347** (2), 280–290. doi:10.1016/j.cej.2018.04.087.

Vogel, B. 2018 *Denitrification as A Sink of N2O Emissions in Side-Stream Treatment – Model Extension and Application ('Denitrifikation als Senke von N2O-Emissionen bei der Teilstrombehandlung – Modellerweiterung und -Anwendung')*. Publications of the Institute of Sanitary Engineering and Waste Management of the Leibniz University, Hannover, Germany. Available from: https://www.tib.eu/de/suchen/id/TIBKAT:1036448681/Denitrifikation-als-Senke-von-N2O-Emissionen-bei?cHash=11f5561c35009105cb3a8b3b68b80516.

Wang, G. T.-Y. & Bryers, J. D. 1997 A dynamic model for receptor-mediated specific adhesion of bacteria under uniform shear flow. *Biofouling* **11** (3), 227–252. doi:10.1080/08927019709378333.

Ye, L., Porro, J. & Nopens, I. 2022 *Quantification and Modelling of Fugitive Greenhouse Gas Emissions From Urban Water Systems*. Chapter 7.3.5 IWA Publishing. doi:10.2166/9781789060461.

Yoon, H., Song, M. J. & Yoon, S. 2017 Design and feasibility analysis of a self-sustaining biofiltration system for removal of low concentration N2O emitted from wastewater treatment plants. *Environmental Science & Technology* **51** (18), 10736–10745. doi:10.1021/acs.est.7b02750.